29 January 1999

ELSEVIER

Chemical Physics Letters 300 (1999) 213–220

CHEMICAL PHYSICS LETTERS

Identification and mobility of deuterated residues in peptides and proteins by $^{2}H-^{13}C$ solid-state NMR

Dick Sandström [1], Mei Hong, Klaus Schmidt-Rohr *

Department of Polymer Science and Engineering, University of Massachusetts at Amherst, Amherst, MA 01003, USA

Received 10 July 1998; in final form 27 October 1998

Abstract

We present a solid-state NMR approach for ^{13}C chemical-shift identification and ^{2}H lineshape characterization of amino-acid residues in peptides and proteins deuterated by amide hydrogen/deuteron exchange. The technique exploits heteronuclear $^{13}C-^{2}H$ dipolar couplings to correlate ^{13}C nuclei and nearby deuterons. Magic-angle spinning provides high sensitivity and ^{13}C chemical-site resolution. The simplest version of the experiment, which is closely related to REDOR, yields a ^{13}C spectrum permitting identification of the deuterated residues. In the full two-dimensional experiment, segmental dynamics are characterized in terms of ^{2}H-NMR lineshapes. The technique is demonstrated on dipeptides and a 14-kDa protein, with ^{13}C in natural abundance. © 1999 Elsevier Science B.V. All rights reserved.

1. Introduction

The understanding of water–protein interactions is of great interest in biochemistry. In membrane-bound proteins, for example, it is useful to know which sites are exposed to water and to what degree they are mobile, since this gives valuable information on the overall organization of the polypeptide chain across and on the cell membrane. The two most important experimental techniques for studying protein hydration have been solution-state NMR and X-ray diffraction (XRD). In particular, the combination of multi-dimensional NMR and amide hydrogen exchange has proven to be a powerful tool for investigating solvent accessibility and protein folding in solution [1,2]. The rates at which the amide hydrogens exchange vary from reciprocal milliseconds to reciprocal weeks/months [3]. The longest values are observed for amides involved in strong hydrogen bonds in regular secondary structures. Unfortunately, neither solution-state NMR nor XRD are feasible when the macromolecules are immobilized in membranes, tumble slowly, or tend to aggregate without forming well-defined crystals. In solid-state NMR studies of biological systems, hydrogen/deuteron (H/D) exchange has also been exploited by several groups [4,5], but these studies usually involve examinations of one-dimensional ^{2}H spectra without the chemical-site resolution that is crucial for the detailed investigation of complex biomolecules.

In this Letter, we report a novel solid-state NMR approach that determines the D_2O-accessibility of

* Corresponding author. E-mail: srohr@polysci.umass.edu

[1] On leave from the Division of Physical Chemistry, Arrhenius Laboratory, Stockholm University, Sweden.

0009-2614/99/$ - see front matter © 1999 Elsevier Science B.V. All rights reserved.
PII: S0009-2614(98)01325-6

various parts of a peptide or protein in the solid or membrane-bound state. More precisely, the aim is to identify and characterize ^{13}C sites close to amide groups that have been deuterated by H/D exchange between D_2O and the amide protons. The experiments utilize the heteronuclear dipole–dipole coupling between ^{13}C and ^{2}H, and operate under magic-angle spinning (MAS) conditions. While MAS provides the required sensitivity and chemical-shift resolution, it also averages out the weak (< 500 Hz) ^{13}C–^{2}H interaction [6]. Borrowing ideas from the REDOR scheme [7], the dipolar coupling is reintroduced by a suitably designed train of rotor-synchronized π pulses. In the one-dimensional (1D) version of the experiment, the ^{13}C chemical-shift spectrum in the detection period identifies the deuterated amino-acid residues. In the full two-dimensional (2D) experiment, the ^{2}H-quadrupolar line shape in the first dimension is used to characterize the mobility [8] of each deuterated residue that has a resolved ^{13}C chemical-shift peak in the second dimension. The new solid-state NMR technique is demonstrated on the following samples: (i) a mixture of deuterated Ala-Gly and unlabeled Phe-Val, (ii) neat, deuterated Ala-Gly, and (iii) deuterated lysozyme. In all cases, natural-abundance ^{13}C signal is detected.

2. Experimental

The three compounds, Ala-Gly (146 Da), Phe-Val (264 Da) and chicken egg-white lysozyme (14 kDa), were purchased from Sigma-Aldrich and used without further purification. Deuterated Ala-Gly was prepared by dissolving 250 mg of the dipeptide in 4 ml of D_2O at 20°C. The solution was then dried under reduced pressure for 24 h. Exchangeable sites on lysozyme were deuterated by dissolving 275 mg of the protein in 3 ml of D_2O at 30°C. Excess solvent was subsequently removed by drying over P_2O_5 for 8 days. The weight of the NMR samples was 65–95 mg.

The NMR experiments were performed at a field of 7.0 Tesla on a Bruker DSX300 spectrometer using a 4 mm triple-resonance MAS probe. Typical radio-frequency field strengths were 105 kHz for ^{1}H decoupling, 60 kHz for ^{13}C and 75 kHz for ^{2}H. ^{1}H–^{13}C cross-polarization (CP) times of 1.5–3.0 ms were used. All spectra were acquired at a rotation frequency of $\omega_r/2\pi = 4000$ Hz at room temperature.

3. Implementation

One-dimensional ^{13}C MAS spectra for determining spatial proximities between ^{13}C and ^{2}H spins are obtained with the pulse sequence shown in Fig. 1a. The scheme starts with conventional cross-polarization from ^{1}H to create enhanced ^{13}C transverse magnetization. This evolves over an even number of rotor periods N containing $2N-2$ rotor-synchro-

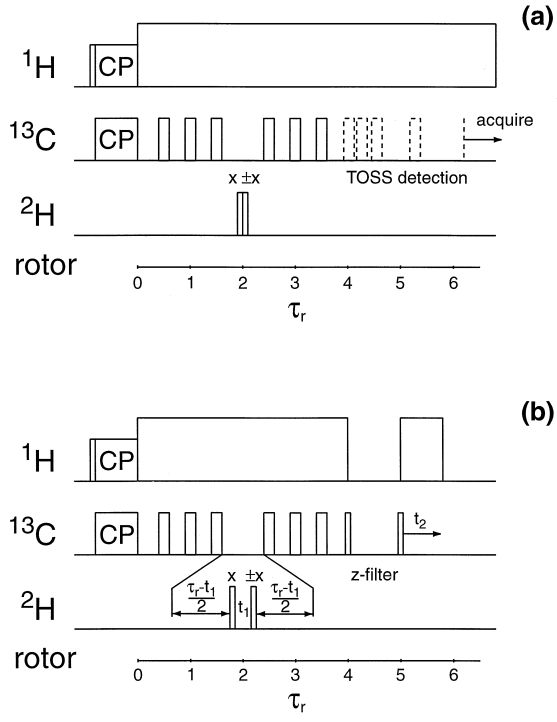

Fig. 1. Pulse sequences for ^{13}C–^{2}H correlation/separation spectroscopy in solids under MAS conditions. (a) Basic one-dimensional version in which a difference signal from experiments with and without the ^{2}H π pulse (implemented by $\pi/2$ pulses as indicated) is recorded. Except for the optional TOSS detection, the ^{13}C pulse train is identical to a ^{13}C–^{15}N REDOR technique previously reported by Garbow and Gullion [9]. The π pulses are phase cycled according to *XY-n* schemes that compensate for pulse imperfections [22]. The illustration contains four rotor periods of dipolar evolution ($N = 4$). However, N can have any even integer value. (b) Two-dimensional sequence for establishing ^{13}C–^{2}H correlation. During the evolution period t_1, the ^{2}H quadrupolar interaction modulates the heteronuclear zero- and double-quantum coherences.

nized ^{13}C π pulses separated by $\tau_r/2$ ($\tau_r = 2\pi/\omega_r$). The ^{13}C π pulse at the center of the evolution period is omitted. In the absence of pulses on ^2H, this ^{13}C pulse train refocuses ^{13}C isotropic chemical shifts, chemical-shift anisotropies and heteronuclear dipolar couplings, and a full rotational echo occurs at $N\tau_r$ [9]. However, if a ^2H π pulse is applied at $N\tau_r/2$ the ^{13}C–^2H dipolar interaction is reintroduced and the refocusing at the end of the evolution period is incomplete. The amount of dephasing is a function of N, ω_r and the strength of the dipolar coupling [10,11]. The ^2H π pulse has been split into two $\pi/2$ pulses. On alternate transients of the experiment, the two $\pi/2$ pulses have either the same or opposite phase. This corresponds to applying either a π pulse or a zero degree pulse. Signal subtraction results in a ^{13}C spectrum that only contains peaks from ^{13}C spins that are coupled to ^2H spins (see below).

The ^{13}C MAS spectrum of a biomolecular system is often very crowded and it is advantageous to reduce the signal overlap as much as possible. Therefore, we have included a total suppression of spinning sidebands (TOSS) [12,13] sequence before acquisition to remove the sidebands that would otherwise have complicated the assignments of the isotropic chemical shifts.

By extending this method to two spectral dimensions, the mobility of the deuterated segments can be studied through the envelope of the ^2H pattern in the first dimension, at their ^{13}C isotropic chemical shifts in the second dimension. The pulse sequence used for achieving this 2D ^2H–^{13}C correlation under MAS is shown in Fig. 1b. It can be considered as a solid-state ^2H–^{13}C HMQC [14,15] experiment with dipolar recoupling during the multiple-quantum excitation and reconversion periods. During the variable evolution period t_1, transverse ^2H coherence is allowed to evolve under the quadrupolar interaction. The duration between the ^2H $\pi/2$ pulse and the adjacent ^{13}C π pulse is contracted in concert with the t_1 incrementation so as to keep the interval between the two central ^{13}C pulses constant and equal to one rotor period. This guarantees a ^{13}C echo at $N\tau_r$. A z-filter preceding the detection period t_2 ensures a purely absorptive spectrum. The two-dimensional cosine data set is processed according to standard procedures to yield a purely absorptive 2D spectrum that is symmetric around $\omega_1 = 0$ [6].

4. Theoretical background

Before presenting the experimental results, we will briefly discuss the theory of the carbon–deuterium MAS experiments involving an ensemble of isolated ^{13}C–^2H pairs. Carbon-13 spins will be denoted by S and deuterons by L.

We start by considering the full 2D pulse scheme in Fig. 1b. Using product operator calculations [16] and the special properties of matrix representations of spin-1 operators, one obtains the following expression for the density operator after zero- and double-quantum excitation/reconversion during a period $N\tau_r$ ($N = 4$ in Fig. 1)

$$\begin{aligned}\sigma_{\pm}(N\tau_r) = {} & S_x\left(\mathbf{1}_L - L_z^2\right) + S_x L_z^2 \cos\Phi'_D \cos\Phi''_D \\ & + S_y L_z \cos\Phi'_D \sin\Phi''_D \\ & \mp S_x L_z^2 \sin\Phi'_D \sin\Phi''_D \cos\Phi_Q(t_1) \\ & \pm S_y L_z \sin\Phi'_D \cos\Phi''_D \cos\Phi_Q(t_1) \quad (1)\end{aligned}$$

where only the single-quantum coherences have been retained. The subscript $\pm$ refers to the phase of the second ^2H $\pi/2$ pulse. After a z-filter of duration τ_r, this simplifies to

$$\begin{aligned}\sigma_{\pm}(N\tau_r + \tau_r) = {} & S_x\left(\mathbf{1}_L - L_z^2\right) + S_x L_z^2\left[\cos\Phi'_D \cos\Phi''_D\right. \\ & \left. \mp \sin\Phi'_D \sin\Phi''_D \cos\Phi_Q(t_1)\right]. \quad (2)\end{aligned}$$

Dephasing that occurs due to transverse spin relaxation has been ignored, except during the z-filter when the proton decoupling is switched off. Modulations from the heteronuclear ^{13}C–^2H dipolar coupling during t_1 can safely be neglected due to the much stronger quadrupolar interaction. The accumulated phase angles in Eqs. (1) and (2) are given by

$$\begin{aligned}\Phi'_D = {} & -(N-1)\int_0^{\tau_r/2} 2\omega_D(t)\,dt \\ & + \int_{\tau_r/2}^{\tau_r - t_1/2} 2\omega_D(t)\,dt, \quad (3)\end{aligned}$$

$$\Phi''_D = (N-1)\int_{\tau_r/2}^{\tau_r} 2\omega_D(t)\,dt - \int_{t_1/2}^{\tau_r/2} 2\omega_D(t)\,dt, \quad (4)$$

$$\Phi_{\mathrm{Q}}(t_1) = \int_{-t_1/2}^{t_1/2} \omega_{\mathrm{Q}}(t)\,\mathrm{d}t, \tag{5}$$

where $\omega_{\mathrm{D}}(t)$ and $\omega_{\mathrm{Q}}(t)$ are the time-dependent ^{13}C–^{2}H dipolar and ^{2}H quadrupolar frequencies, respectively. Explicit expressions for these quantities can be found elsewhere [17]. In Eqs. (3) and (4), the factor of 2 in front of ω_{D} reflects the fact that the dipolar splitting produced by a spin-1 nucleus is twice that of a spin-1/2 nucleus with the same gyromagnetic ratio.

After the basic two-step HMQC phase cycle described in Section 3, from Eq. (2) we obtain the following difference density operator

$$\begin{aligned}\Delta\sigma(N\tau_{\mathrm{r}}+\tau_{\mathrm{r}}) &= \sigma_{-}(N\tau_{\mathrm{r}}+\tau_{\mathrm{r}}) - \sigma_{+}(N\tau_{\mathrm{r}}+\tau_{\mathrm{r}}) \\ &= 2S_x L_z^2 \sin\Phi'_{\mathrm{D}} \sin\Phi''_{\mathrm{D}} \cos\Phi_{\mathrm{Q}}(t_1)\,.\end{aligned} \tag{6}$$

The t_1-dependent modulation of the signal, $\cos\Phi_{\mathrm{Q}}(t_1)$, after powder averaging and Fourier transformation produces a ^{2}H-quadrupolar wideline spectrum. If the maximum t_1 value is $\leqslant \tau_{\mathrm{r}}/2$, this spectrum is the envelope of the ^{2}H MAS NMR sideband pattern obtained at the chosen spinning speed.

In this two-dimensional solid-state HMQC experiment, the crucial terms in the density operator develop through heteronuclear multiple-quantum coherences that evolve under the ^{2}H quadrupolar coupling during t_1. It is clear that only ^{13}C spins coupled to ^{2}H spins will contribute to the observed NMR spectrum since the amplitude-modulated signal of Eq. (6) vanishes if ω_{D} is identically zero or negligibly small. When t_1 is set to zero, one can alternatively calculate the observed ^{13}C signal without considering multiple-quantum coherences, by just taking into account the dephasing of the observable magnetization, which is coupled with the generation of heteronuclear single-quantum coherences. This is the approach taken in the conventional treatment of REDOR [18]. In fact, the 1D pulse sequence in Fig. 1a corresponds to a ^{13}C-detected ^{13}C–^{2}H REDOR experiment, with the subtraction of the partly dephased signal from the reference signal directly implemented in the phase cycle. By setting $t_1 = 0$, we obtain $\Phi_{\mathrm{Q}}(t_1) = 0$ and $\Phi'_{\mathrm{D}} = \Phi''_{\mathrm{D}} = N/2\,\Delta\Phi$, with the phase $\Delta\Phi$ acquired in one rotor period given by

$$\begin{aligned}\Delta\Phi &= -2\int_0^{\tau_{\mathrm{r}}/2} 2\,\omega_{\mathrm{D}}(t)\,\mathrm{d}t \\ &= -\frac{2\sqrt{2}\,R\tau_{\mathrm{r}}}{\pi}\sin 2\beta\sin\gamma, \\ R &= -\frac{\mu_0}{4\pi}\hbar\frac{\gamma_{\mathrm{L}}\gamma_{\mathrm{S}}}{r_{\mathrm{LS}}^3}\,.\end{aligned} \tag{7}$$

Here, $\{\alpha,\beta,\gamma\}$ is the set of Euler angles relating the orientation of the internuclear vector $\boldsymbol{r}_{\mathrm{LS}}$ to a rotor-fixed axis system. The third angle α is irrelevant for an axially symmetric interaction such as the dipolar coupling. The other symbols in Eq. (7) have their usual meanings [6]. Setting $t_1 = 0$ thus reduces Eq. (1) to

$$\begin{aligned}\sigma_{\pm}(N\tau_{\mathrm{r}}) &= S_x\left(\mathbf{1}_{\mathrm{L}} - \mathrm{L}_z^2\right) \\ &\quad + S_x\mathrm{L}_z^2\cos\left[N/2(\Delta\Phi\pm\Delta\Phi)\right] \\ &\quad + S_y L_z \sin\left[N/2\,(\Delta\Phi\pm\Delta\Phi)\right].\end{aligned} \tag{8}$$

Employing the relationship between the density operator and the time-domain NMR signal, $s_{\pm}(t) \propto \mathrm{tr}\{\sigma_{\pm}(t)S_{+}\}$ with $S_{+} = S_x + \mathrm{i}S_y$, Eq. (8) yields the powder-averaged signal intensities at the start of detection, after a dipolar excitation/reconversion period of duration $N\tau_{\mathrm{r}}$

$$\bar{s}_{-}(N\tau_{\mathrm{r}}) = \int_0^{2\pi}\int_0^{\pi}\frac{s_0}{4\pi}\sin\beta\,\mathrm{d}\beta\,\mathrm{d}\gamma = \langle s_0\rangle = s_0\,, \tag{9}$$

$$\begin{aligned}\bar{s}_{+}(N\tau_{\mathrm{r}}) &= \left\langle s_0\left[\frac{1}{3}+\frac{2}{3}\cos(N\Delta\Phi)\right]\right\rangle \\ &= s_0\left[\frac{1}{3}+\frac{2}{3}\langle\cos(N\Delta\Phi)\rangle\right],\end{aligned} \tag{10}$$

$$\Delta\bar{s}(N\tau_{\mathrm{r}}) = \bar{s}_{-} - \bar{s}_{+} = s_0\frac{2}{3}\left[1-\langle\cos(N\Delta\Phi)\rangle\right], \tag{11}$$

where $s_0 = \mathrm{tr}\{S_x\mathbf{1}_{\mathrm{L}}S_{+}\}$. Eq. (11) is equivalent to the result given by Schmidt et al. [18]. Ignoring relaxation, the long-time value (for $N\tau_{\mathrm{r}}\cdot R \gg 1$) of the REDOR difference signal Eq. (11) is $2s_0/3$. This value should be compared to $2s_0$, which is the signal intensity after two transients without ^{2}H pulses. Thus,

the efficiency at long times $N\tau_r$ is 33%. Evaluating the powder average in Eq. (11), one finds that the maximum efficiency in this experiment is 35%, achieved at $N\tau_r \cdot R = 2\pi \cdot 0.8$ [18].

5. Results and discussion

The 1D version of the method was first demonstrated on a mixture of Ala-Gly deuterated by H/D exchange and unlabeled Phe-Val. Fig. 2a shows the conventional ^{13}C CP/MAS/TOSS spectrum for reference. The spectra resulting from application of the pulse sequence in Fig. 1a, with a total excitation and reconversion time of 10 rotation periods or 2.5 ms, are shown in Fig. 2b,c. These ^{13}C–^{2}H REDOR-TOSS difference spectra contain only signals from the five non-equivalent carbons in deuterated Ala-Gly. Since the Phe-Val dipeptide is not enriched in ^{2}H, all its peaks are suppressed effectively by the phase cycle. Comparison of Fig. 2a,b indicates that the efficiency of the experiment is 16–20%, which compares reasonably well with the theoretical limit of 35% which neglects all relaxation and pulse-excitation effects. In Ala-Gly deuterated by H/D exchange (see structure in Fig. 3), all carbons are separated by two or three bonds from the nearest ^{2}H. The two- and three-bond ^{2}H–^{13}C dipolar coupling constants $R/(2\pi)$ (see Eq. (7)), range from -520 to -200 Hz.

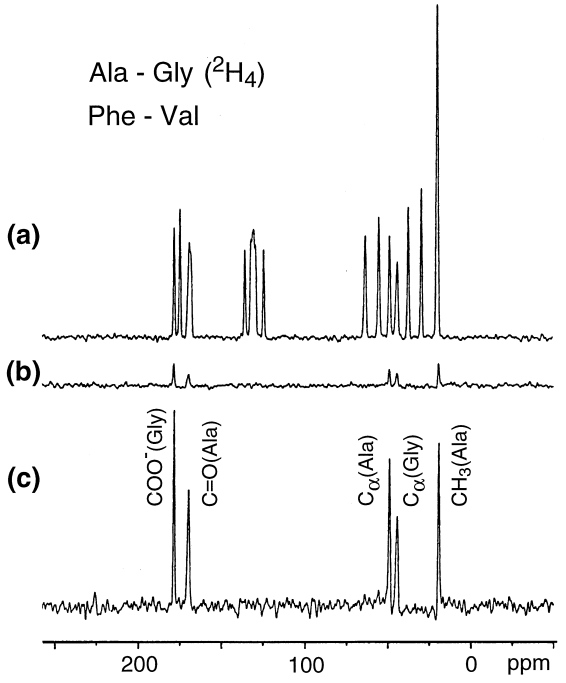

Fig. 2. ^{13}C spectra of a mixture consisting of Ala-Gly deuterated by H/D exchange and unlabeled Phe-Val dipeptides. (a) Regular TOSS spectrum. (b) ^{13}C–^{2}H REDOR difference spectrum obtained using the pulse sequence in Fig. 1a with $N = 10$. The traces in (a) and (b) are averages of 256 transients, corresponding to an experimental time of 15 min. (c) ^{13}C–^{2}H REDOR difference spectrum acquired with 2048 transients, with all other experimental parameters as in (b). The peak assignment of Ala-Gly is based on comparisons with previous ^{13}C chemical-shift studies [23,24].

In principle, the same information could have been obtained by previously reported ^{13}C–^{2}H REDOR schemes [19]. However, the sequence in Fig. 1a has two advantages. First, it involves a minimum number of ^{2}H pulses. This minimizes excitation problems, which are serious here since the ^{2}H quadrupolar coupling can exceed the field strength $\gamma^{2H} B_1^{2H}$. Similar considerations guided the design of the REAPDOR experiment [20]. Second, the signal subtraction is built into the phase cycle, which minimizes potential problems arising from long-term spectrometer drifts.

In Fig. 3, we show a 2D spectrum obtained with the pulse sequence in Fig. 1b from a sample of deuterated Ala-Gly. The projection on the ω_2 axis consists of centerbands from the five carbons in Ala-Gly. Spinning sidebands from the carboxyl and carbonyl carbons are also present since no TOSS was applied before detection. Information about the dynamics of the deuterated sites is obtained by extracting cross-sections parallel to the ω_1 axis that pass through the ^{13}C resonances in ω_2. It is seen that the deuterated segments in Ala-Gly are predominantly of two types: those that exhibit substantial motional narrowing and those that are approximately stationary. The slice through the C_α(Ala) peak is dominated by a ^{2}H signal with a splitting of 25 kHz. A corresponding splitting is observed prominently in conventional 1D ^{2}H NMR spectra of this sample (not shown). The 25 kHz splitting corresponds to a residual quadrupolar coupling constant (qcc) of $4/3 \cdot 25$ kHz $= 33$ kHz and may be attributed to the rotating ND_3^+ group. Datema et al. observed a value of qcc $= 44$ kHz for terminal ND_3^+ groups of ornithine side chains in solid gramicidin S [4].

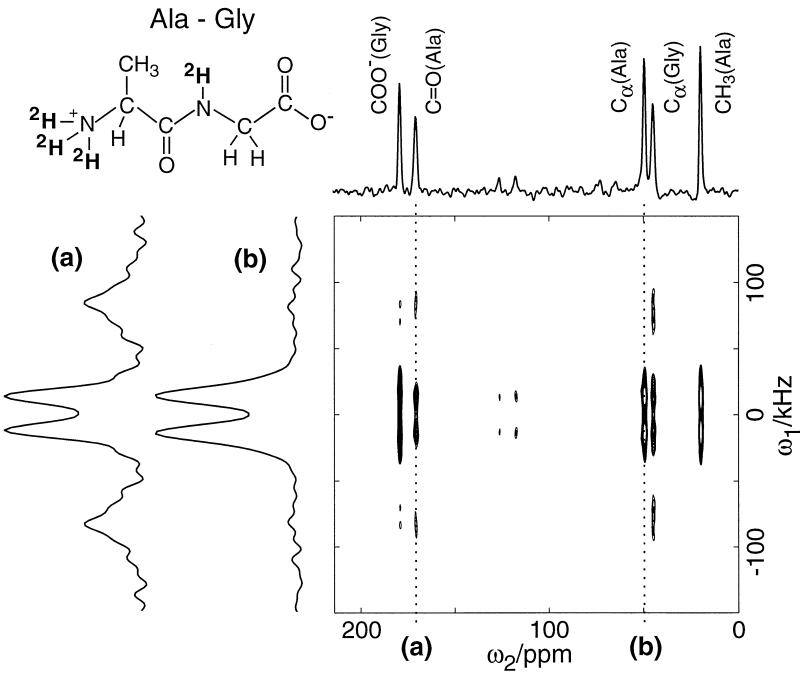

Fig. 3. Two-dimensional ^{2}H-quadrupolar/^{13}C-chemical-shift spectrum of Ala-Gly deuterated by H/D exchange (see structure in inset) obtained by the pulse sequence in Fig. 1b with $N = 8$. In (a) and (b), we show ^{2}H-quadrupolar cross-sections along the ω_1 axis that run through the peptide carbonyl and C_α(Ala) centerbands in ω_2, respectively. The 2D data set consisted of 40×2048 points and the t_1 incrementation time was 2.0 μs. For each t_1 value, 416 transients were recorded (total acquisition time of 14 h).

The broader component (e.g. in the slice through the carbonyl carbon of the peptide group) is characterized by a quadrupolar coupling constant of around 210 kHz. This qcc is similar to those obtained from rigid amide N-^{2}H sites in lysozyme [21] (qcc = 210 kHz), gramicidin A and S [4] (qcc = 200 kHz), and poly-γ-benzyl-L-glutamate [5] (qcc = 202 kHz). A closer inspection of the cross-section shown in Fig. 3 indicates that the lineshape of the amide deuteron deviates from the ideal Pake pattern [6]. A number of factors is responsible for this deviation. One reason is that for N-^{2}H deuterons, the asymmetry parameter does not vanish, but rather $\eta \approx 0.25$ [21]. Secondly, the ^{2}H spectrum was acquired under MAS. Thus, it represents the envelope of the sideband pattern, which at the rotation rate of 4000 Hz is not exactly identical to the static powder pattern. Third, a 'dead-time' or excitation problem exists due to finite ^{2}H pulse lengths. The two pulses of 2 μs duration that define the start and the end of the evolution time produce an effective dead time of 2 μs. This results in a characteristic depression of the center of the spectrum, however, without significantly affecting the position of the two horns.

It is difficult to trace out all intra- and intermolecular connectivities between ^{13}C and ^{2}H spins as would be required to quantify the broad and narrow ^{2}H signal contributions in a given slice of the 2D spectrum in Fig. 3. It is, however, interesting to note that the strongest signals from the broad ^{2}H component are observed for the peptide carbonyl and C_α(Gly) carbons. These sites are closest to the amide group, which imparts confidence in the suggested assignment of the broad powder pattern to the rigid amide N-^{2}H group. It is reassuring to observe that the ^{13}C–^{2}H transfer is efficient even in the presence of large-amplitude motions that average the qcc significantly. This indicates that the method is indeed suitable for characterizing site mobility.

Fig. 4 demonstrates applications of the 1D version of the experiment to lysozyme, a 14-kDa globular protein, deuterated by H/D exchange. The regular

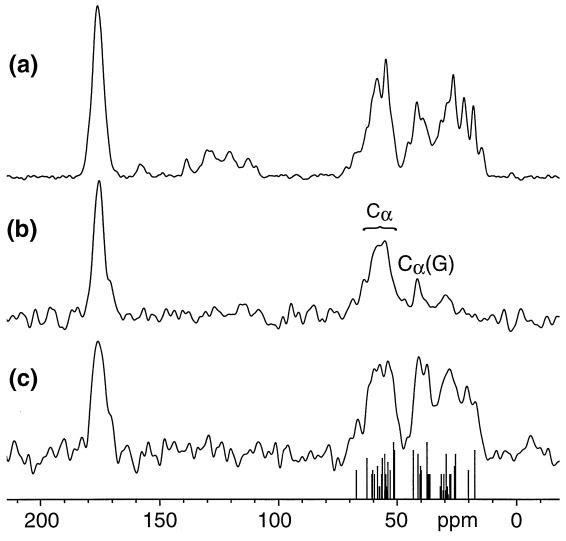

Fig. 4. Natural-abundance ^{13}C spectra of lysozyme deuterated by H/D exchange. (a) TOSS spectrum. (b) and (c) show spectra obtained using the pulse scheme in Fig. 1a with $N = 4$ and $N = 10$, respectively. At the bottom, typical frequency positions of carbons within three bonds from deuterons are indicated by vertical lines, whose height indicates the abundance of the sites in lysozyme. Acquisition of the spectrum in (a) took 102 min (2048 transients), while the spectra in (b) and (c) each required 31 h of instrument time (37824 transients).

CP/MAS/TOSS spectrum shown in Fig. 4a is compared with ^{13}C–^{2}H REDOR-TOSS difference spectra (Fig. 4b,c) obtained using the pulse sequence in Fig. 1a with $N = 4$ and $N = 10$ cycles, respectively. At a short excitation/reconversion time ($N\tau_r = 1$ ms), only two-bond ^{2}H–^{13}C couplings produce significant signal intensity. As expected, in the resulting spectrum (Fig. 4b), one observes only the carbonyl signal around 175 ppm, the C_α band of 50–65 ppm, the C_α(Gly) peak at 43 ppm, and a small signal in the C_β chemical-shift region. Peaks from carbons close to side-chain residues that contain exchangeable hydrogens are also present. At a longer time of $N\tau_r = 2.5$ ms, two- and three-bond couplings are excited, so that C=O, C_α, and C_β signals are observable. Again, ^{13}C sites in sidegroups near $N^{2}H_n$ and $O^{2}H$ moieties also produce significant signal intensity. It is found that the observed positions of the upfield peaks in Fig. 4c match qualitatively with the densest regions in the frequency distribution of carbons located within three bonds from deuterons. The frequency distribution was extracted from the literature [3], and is indicated at the bottom of the spectrum in Fig. 4 by vertical lines.

A closer inspection of the spectrum in Fig. 4c compared to that of Fig. 4a reveals an increased relative height of the C_β signals near 42 ppm relative to the C_α peaks at 50 ppm and differences in the finer features of the C_α band. This probably reflects differences in the level of deuteration of the various residue types. For a more detailed analysis, resonance assignment using 2D NMR techniques [25] would be necessary. This requires ^{13}C and ^{15}N labeling, [26] which would also increase the sensitivity by one to two orders of magnitude.

If efficient cross-polarization (CP) from ^{2}H to ^{13}C could be achieved under MAS, it would allow for alternative implementations of the experiments described in this Letter. In non-spinning liquid-crystalline samples, one-bond ^{2}H–^{13}C CP has recently been demonstrated and put to good use for measuring site-resolved C-^{2}H bond order parameters in perdeuterated molecules with high precision [27]. However, it was concluded that this approach works well only for ^{2}H quadrupolar couplings reduced by fast anisotropic molecular motions [28]. In rigid solids, the quadrupolar coupling constant of up to $2\pi \cdot 200$ kHz exceeds the practically achievable ^{2}H radiofrequency strength γB_1 and the ^{2}H–^{13}C CP approach with its several milliseconds of B_1-irradiation becomes impractical, in particular for the weak two- and three-bond ^{2}H–^{13}C couplings of interest in amide-deuterated peptides and proteins. It should also be noted that the observed magnetization originates from protons (due to the ^{1}H–^{13}C CP at the start of the experiment) in the HMQC approach presented here, but from deuterons in the ^{2}H–^{13}C CP-approach. This results in a sensitivity advantage of $\gamma_{^1H}/\gamma_{^2H} = 6.4$ in our approach.

6. Conclusions

We have reported a solid-state NMR method for identification and characterization of ^{13}C sites in peptides and proteins that are close to deuterons which are introduced by amide H/D exchange from D_2O. The MAS technique exploits the recoupled dipolar interactions between ^{13}C spins and ^{2}H spins separated by several bonds. In the 1D version, the

^{13}C spectrum of the carbons within a certain distance from any of the deuterons is observed. The full 2D experiment provides information about the mobility of the deuterated residues in terms of the ^{2}H-quadrupolar powder line shape. For oligopeptides with ^{13}C in natural abundance, the signal-to-noise ratio was shown to be satisfactory even in the 2D experiment. The 1D spectra obtained for ^{13}C-unlabeled lysozyme suggest that with the significant sensitivity enhancement achievable by ^{13}C-labeling, the technique will be applicable to membrane-bound proteins.

Acknowledgements

This work was supported by a Beckman Young Investigator Award to KS-R. DS gratefully acknowledges financial support from the Wenner-Gren Center Foundation and the Foundation Blanceflor Boncompagni-Ludovisi, née Bildt.

References

[1] G. Wagner, K. Wüthrich, J. Mol. Biol. 160 (1982) 343.
[2] S.E. Radford, C.M. Dobson, P.A. Evans, Nature 358 (1992) 302.
[3] J.N.S. Evans, Biomolecular NMR Spectroscopy, Oxford University Press, Oxford, 1995.
[4] K.P. Datema, K.P. Pauls, M. Bloom, Biochemistry 25 (1986) 3796.
[5] M.G. Usha, R.J. Wittebort, J. Mol. Biol. 208 (1989) 669.
[6] K. Schmidt-Rohr, H.W. Spiess, Multidimensional Solid-State NMR and Polymers, Academic Press, London, 1994.
[7] T. Gullion, J. Schaefer, J. Magn. Reson. 81 (1989) 196.
[8] H.W. Spiess, Adv. Polym. Sci. 66 (1985) 23.
[9] J.R. Garbow, T. Gullion, J. Magn. Reson. 95 (1991) 442.
[10] T. Gullion, J. Schaefer, Adv. Magn. Reson. 13 (1989) 57.
[11] K.T. Mueller, T.P. Jarvie, D.J. Aurentz, B.W. Roberts, Chem. Phys. Lett. 242 (1995) 535.
[12] W.T. Dixon, J. Chem. Phys. 77 (1982) 1800.
[13] W.T. Dixon, J. Schaefer, M.D. Sefcik, E.O. Stejskal, R.A. McKay, J. Magn. Reson. 49 (1982) 341.
[14] L. Müller, J. Am. Chem. Soc. 101 (1979) 4481.
[15] A. Bax, R.H. Griffey, B.L. Hawkins, J. Magn. Reson. 55 (1983) 301.
[16] O.W. Sørensen, G.W. Eich, M.H. Levitt, G. Bodenhausen, R.R. Ernst, Progr. NMR Spectrosc. 16 (1983) 163.
[17] M.M. Maricq, J.S. Waugh, J. Chem. Phys. 70 (1979) 3300.
[18] A. Schmidt, R.A. McKay, J. Schaefer, J. Magn. Reson. 96 (1992) 644.
[19] A. Schmidt, T. Kowalewski, J. Schaefer, Macromolecules 26 (1993) 1729.
[20] T. Gullion, Chem. Phys. Lett. 246 (1995) 325.
[21] S. Schramm, E. Oldfield, Biochemistry 22 (1983) 2908.
[22] T. Gullion, D.B. Baker, M.S. Conradi, J. Magn. Reson. 89 (1990) 479.
[23] H. Saito, Magn. Reson. Chem. 24 (1986) 835.
[24] Z. Gu, R. Zambrano, A. McDermott, J. Am. Chem. Soc. 116 (1994) 6368.
[25] M. Hong, R.G. Griffin, J. Am. Chem. Soc. 120 (1998) 7113.
[26] M. Hong (submitted).
[27] C. Auger, A. Lesage, S. Caldarelli, P. Hodgkinson, L. Emsley, J. Phys. Chem. 102 (1998) 3718.
[28] P. Hodgkinson, C. Auger, L. Emsley, J. Chem. Phys. 109 (1998) 1873.